Controllable strain-induced uniaxial anisotropy of Fe81Ga19 films deposited on flexible bowed-substrates

Guohong Dai, Qingfeng Zhan, Huali Yang, Yiwei Liu, Xiaoshan Zhang, Zhenghu Zuo, Bin Chen, and Run-Wei Li

---

Articles you may be interested in

Magneto-elastic and magnetic domain properties of Fe81Ga19/Si(100) films
J. Appl. Phys. **115**, 013909 (2014); 10.1063/1.4861160

Effect of buffer layer and external stress on magnetic properties of flexible FeGa films
J. Appl. Phys. **113**, 17A901 (2013); 10.1063/1.4793602

Effect of mechanical strain on magnetic properties of flexible exchange biased FeGa/IrMn heterostructures
Appl. Phys. Lett. **102**, 022412 (2013); 10.1063/1.4776661

Mechanically tunable magnetic properties of Fe81Ga19 films grown on flexible substrates
Appl. Phys. Lett. **100**, 122407 (2012); 10.1063/1.3696887

Stress annealing of Fe–Ga transduction alloys for operation under tension and compression
J. Appl. Phys. **97**, 10M301 (2005); 10.1063/1.1845933

Controllable strain-induced uniaxial anisotropy of $Fe_{81}Ga_{19}$ films deposited on flexible bowed-substrates

Guohong Dai,[1,2,3] Qingfeng Zhan,[1,2,a)] Huali Yang,[1,2] Yiwei Liu,[1,2] Xiaoshan Zhang,[1,2] Zhenghu Zuo,[1,2] Bin Chen,[1,2] and Run-Wei Li[1,2,b)]

[1]*Key Laboratory of Magnetic Materials and Devices, Ningbo Institute of Material Technology and Engineering, Chinese Academy of Sciences, Ningbo 315201, People's Republic of China*
[2]*Zhejiang Province Key Laboratory of Magnetic Materials and Application Technology, Ningbo Institute of Material Technology and Engineering, Chinese Academy of Sciences, Ningbo 315201, People's Republic of China*
[3]*School of Science, Nanchang University, Nanchang 330031, People's Republic of China*

We propose a convenient method to induce a uniaxial anisotropy in magnetostrictive $Fe_{81}Ga_{19}$ films grown on flexible polyethylene terephthalate (PET) substrates by bending the substrate prior to deposition. A tensile/compressive stress is induced in the $Fe_{81}Ga_{19}$ films when PET substrates are shaped from concave/convex to flat after deposition. The stressed $Fe_{81}Ga_{19}$ films exhibit a significant uniaxial magnetic anisotropy due to the internal stress arising from changes in shape of PET substrates. The easy axis is along the tensile stress direction and the coercive field along easy axis is increased with increasing the internal tensile stress. The remanence of hard axis is decreased with increasing the compressive stress, while the coercive field is almost unchanged. A modified Stoner-Wohlfarth model with considering the distribution of easy axes in polycrystalline films is used to account for the magnetic properties tuned by the strain-controlled magnetoelastic anisotropy in flexible $Fe_{81}Ga_{19}$ films. Our investigations provide a convenient way to induce uniaxial magnetic anisotropy, which is particularly important for fabricating flexible magnetoelectronic devices. © 2013 AIP Publishing LLC. [http://dx.doi.org/10.1063/1.4829670]

I. INTRODUCTION

Due to the development of sensors and actuators in microelectromechanical systems (MEMS), the interest in magnetostrictive thin films has rapidly grown in recent years.[1–4] The magnetic anisotropy of magnetostrictive films is one of the most important properties in determining the sensitivity function of sensors or reducing the necessary driving magnetic fields of actuators.[5] Magnetic anisotropy in magnetostrictive materials can be produced by the mechanical stresses due to the magneto-elastic coupling.[6] Therefore, mechanical stress can be used as an effective way to produce desired anisotropies in magnetostrictive thin films along a particular direction, which can be applied in magnetic sensors and actuators.[7] For example, in giant magnetoresistance (GMR) multilayers and spin-valve structures,[8–12] the magnetoresistance is sensitive to the relative orientation of magnetization in two neighboring ferromagnetic (FM) films. An externally applied stress may change the geometry of magnetic anisotropy in magnetostrictive multilayers through inverse magnetostriction (Villary) effect, and thus tune their transport properties. Therefore, introducing a controllable magnetic anisotropy in thin films is an interesting topic for both fundamental researches and potential practical applications. There are several effective methods to induce magnetic anisotropy, such as, field annealing treatments,[13] lattice mismatch strain,[14] and ripple-like structures produced by ion

sputter etching,[15] etc. In previous studies, Garcia et al. introduced a sputtering technique on bowed glass substrates to induce a controllable magnetic anisotropy in FeB/CoSiB bilayers.[16,17] Using stress anneal growth, Tan et al. investigated the magnetic anisotropy of $Tb_{0.4}Fe_{0.6}$, $Fe_{0.5}Co_{0.5}$ single layer films and $[Tb_{0.4}Fe_{0.6}/Fe_{0.5}Co_{0.5}]_n$ multilayers deposited on Si substrates.[3] Compared to the field annealing and intrinsic stress induced anisotropy, this stress anneal induced anisotropy has much larger magnitude and the direction could also be controlled. However, the clamping effect caused by stiff substrates may reduce the magneto-elastic coupling and the induced anisotropy in magnetostrictive thin films. On the other hand, an additional complicated apparatus is required to bow the stiff substrates, and the induced strain is still rather small (only $\sim 6 \times 10^{-6}$) for practical application.

Recently, flexible magnetic films and spintronic devices grown on plastic substrates which can be shaped into almost any arbitrary geometry have attracted much attention.[18,19] When applying mechanical stress, flexible magnetic films can be freely deformed, so that the magnetoelastic coupling is obviously enhanced. The thin films deposited onto flexible substrates are useful in stretchable magnetoelectronics[18] and high-frequency electromagnetic devices due to their stress sensitivity.[20] For practical applications, such as microwave filters and absorbers, the resonance frequency is correlated with the stress-induced magnetic anisotropy.[21] Besides, the ability to generate a tunable anisotropy via prestress of flexible-substrate bending can eliminating the need for complicated field-annealing processes and the clamping effect which produced by stiff substrate. Therefore, magnetostrictive films

---

a)Electronic mail: zhanqf@nimte.ac.cn.
b)Electronic mail: runweili@nimte.ac.cn.

deposited on flexible substrates are suitable for study the correlation between magnetism and external stress. $Fe_{81}Ga_{19}$ is a positive magnetostrictive alloy, which exhibits moderate magnetostriction ($\sim$350 ppm for Ga content of 19%) under very low magnetic fields ($\sim$100 Oe) but good mechanical properties.[22] Previously, we have reported that a mechanical stress produced by bending substrates was employed to change the geometry of anisotropy in flexible $Fe_{81}Ga_{19}$ grown on polyethylene terephthalate (PET) and tune the squareness of hysteresis loops.[23] So far, the influences of mechanical stress, applied during fabrication, on magnetic anisotropy and coercive field have been rarely studied in flexible magnetic films. In this work, we deposited 50-nm-thick magnetostrictive $Fe_{81}Ga_{19}$ films on bowed flexible PET substrates. Due to the induced internal stress arising from flattening the substrates from a bowed status, a controllable uniaxial magnetic anisotropy is induced in $Fe_{81}Ga_{19}$ films. The coercive field can be significantly tuned by adjusting the bending strain of substrates during sputtering. The magnetic behaviors of $Fe_{81}Ga_{19}$ films with bowed-substrate-induced magnetic anisotropy can be qualitatively interpreted by a modified Stoner-Wohlfarth model.

II. EXPERIMENTAL

Using direct current magnetron sputtering method, we fabricated 50-nm-thick $Fe_{81}Ga_{19}$ films on bowed flexible 156-μm-thick PET substrates at room temperature. Before the substrates were transferred into the sputtering chamber, they have been cleaned in ethyl alcohol using ultrasonic agitation for 15 min and then blow-dried with nitrogen gas. In order to induce a homogeneous strain, we bowed the substrates by directly fixing the PET substrates onto the concave or convex surface of aluminum alloy molds, as shown in Figs. 1(a) and 1(c), respectively. The strain in the films can be adjusted by changing the curvature radius of the molds. The base pressure of the sputtering chamber was in the range of 10^{-5} Pa. During sputtering, the argon flow was kept at 50 sccm (standard cubic centimeter per minute) and the pressure was set at 1.0 Pa. A deposition rate of 10.0 nm/min was used for growing $Fe_{81}Ga_{19}$ layers. Prior to being taken out of the vacuum chamber, $Fe_{81}Ga_{19}$ films were capped by a 5-nm-thick Au layer to avoid oxidation. Although the bowed substrates are subjected to strain, the films deposited on them are not stressed until all the samples flattened to a plane. The

applied stress can be effectively transferred to $Fe_{81}Ga_{19}$ films due to the mechanical interlocking and chemical bonding between the $Fe_{81}Ga_{19}$ films and PET substrates.[24] As shown in Figs. 1(b) and 1(d), a tensile or compressive stress is produced in $Fe_{81}Ga_{19}$ films when PET substrates are shaped from concave/convex to flat after deposition. Due to the excellent flexibility of PET substrate (Elastic limit: 50% $\sim$150%) and good ductility of $Fe_{81}Ga_{19}$ films, the strain state of $Fe_{81}Ga_{19}$/PET structure is within elastic limit. The strain, ε, and the stress, σ, are evaluated by using the relations $\varepsilon = t/2\rho$ and $\sigma = \varepsilon E_f/(1-\upsilon^2)$, respectively, where E_f and t are the Young's modulus of $Fe_{81}Ga_{19}$ film and the thickness of the substrate including the film thickness. ρ is the curvature radius of the concave or convex surface of the molds, and υ is the Poisson ratio. ε and σ are considered to be positive/negative for the film subjected to tensile/compressive strain. After releasing the PET substrates off the convex and concave surfaces, the bending-induced strains corresponding to different radii of convex or concave surfaces are -0.26%, -0.23%, -0.18%, -0.09%, $+0.23\%$, $+0.39\%$, and $+0.62\%$. The angular dependence of hysteresis loops for samples with various pre-stresses was measured by vibrating sample magnetometer (VSM, Lakeshore 7410) at room temperature with the magnetic field applied in the plane of film. The field orientation φ is defined as the angle between the magnetic field direction and the induced stress.

III. RESULTS AND DISCUSSIONS

As shown in Fig. 2(a), when the magnetic field is parallel to the internal stress of $Fe_{81}Ga_{19}$ films, i.e., the angle of $\varphi = 0°$, the hard axis of magnetic films is parallel to the compressive stress and the squareness of hysteresis loops is decreased dramatically from 0.52 to 0.28 with increasing the compressive strain from -0.09% to -0.26%. The smooth magnetic switching process around coercivities indicates a coherent rotation of magnetization. Figure 2(b) shows that the values of M_r/M_s for magnetic field perpendicular to the compressive stress are almost unity, indicating the transverse alignment of the magnetic moments under compressive stress. The sharp reversal of magnetization can be interpreted by the nucleation of magnetic domains and rapid displacements of domain walls.[25,26] In Fig. 2(b), the coercive field along the easy axis is enhanced from 38 to 67 Oe with increasing the transverse compressive strain from -0.09% to -0.26%. In contrast, there is almost no change in coercivity measured along the hard axis, as shown in Fig. 2(a). Both the squareness and coercive field versus the in-plane magnetic field angle exhibit a uniaxial symmetry about the easy or hard axes, as, respectively, shown in Figs. 2(c) and 2(d). The maximum M_r/M_s ratio appears at $\varphi = 90°$, indicating that the easy axis is perpendicular to the applied compressive strains. The M_r/M_s ratio is found to oscillate with a periodicity of 180°, corresponding to the stress-induced uniaxial magnetic anisotropy. As seen in Fig. 2(c), with the increase of internal strain from -0.09% to -0.26%, the maximum value of M_r/M_s increases from 0.88 to 0.94 and the minimum M_r/M_s ratio decreases from 0.55 to 0.30, which indicates that the magnetic anisotropy is enhanced by increasing the pre-strain
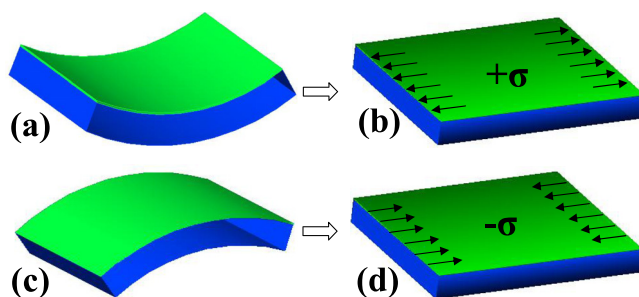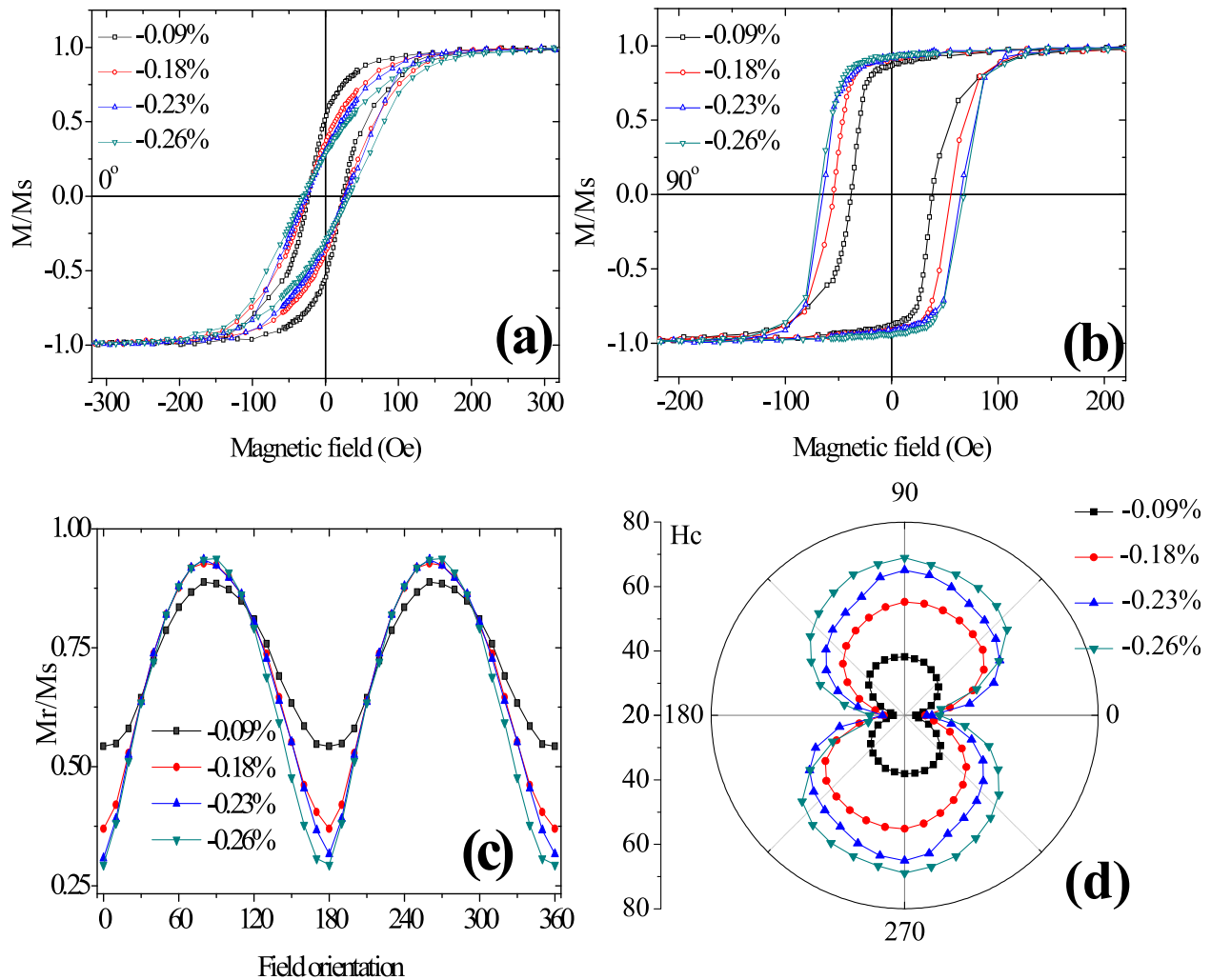

FIG. 1. Schematic show of the bowed-substrates prior to sputtering: (a) up and (c) down bending. After deposition, the stress in magnetic films induced by the substrate recovery are (b) tensile and (d) compressive.

FIG. 2. Representative magnetic hysteresis loops for $Fe_{81}Ga_{19}$/PET with magnetic field applied (a) parallel or (b) perpendicular to the various compressive stresses; (c) Squareness and (d) coercive field versus in-plane field angle for $Fe_{81}Ga_{19}$/PET with different internal stresses.

of the substrate. As shown in Fig. 2(d), the "8" shaped polar plots of coercive field under different compressive strains indicate that the increase of H_c is dependent on the field orientation. Along the easy axis, the increase of H_c is significant, but H_c along the hard axis stay nearly unchanged.

The stress-induced uniaxial anisotropy can be experimentally determined from the energy difference to magnetize the sample along the easy and hard axes. The area between the virgin curve (M-H), the M-axis, and the horizontal line of M_s determines the work done by the magnetic field to saturate the samples. The virgin magnetization curve can be obtained approximately by averaging the left and right branches of the hysteresis loops.[27] Using the relation

$$W = \int_0^{M_s} H(M)dM,$$

where M_s is the experimentally measured saturation magnetization of $Fe_{81}Ga_{19}$ film, we can numerically calculate the work done by the magnetic field to saturate the sample. In our experiment, M_s of $Fe_{81}Ga_{19}$ films is measured about 880 emu/cm^3, which is much less than that of the bulk

counterpart but comparable with the previously reported values in $Fe_{81}Ga_{19}$ films.[28,29] The strain-induced anisotropy is calculated to be increased from 1.42×10^4 to 3.74×10^4 erg/cm^3 with the increase of compressive strain from -0.09% to -0.26%. The change of magnetic anisotropy ΔK_e corresponding to increase of stress $\Delta\sigma$ can be expressed by[30] $\Delta K_e = 3\lambda_s\Delta\sigma/2$, λ_s is the magnetostriction constant. Using Young's modulus $E_f = 60$ GPa for $Fe_{81}Ga_{19}$ film and the typical value $\upsilon = 0.3$ for metals,[31] the saturation magnetostriction constant of $Fe_{81}Ga_{19}$ films can be calculated by the linear fitting determined slope of $\Delta K_e/\Delta\sigma$. The obtained saturation magnetostriction of $\lambda_s = 12.0$ ppm is much smaller than the quoted value of 100 ppm for $Fe_{81}Ga_{19}$ films.[32] Compared to the high magnetostriction in $Fe_{81}Ga_{19}$ single crystals, λ_s has been found to be significantly decreased in sputtered FeGa films due to the significant interface contribution to effective magnetostriction.[33] This convenient and accurate method can be applied to measure the magnetostrictive coefficient in flexible thin films.

Figures 3(a) and 3(b) show the hysteresis curves for $Fe_{81}Ga_{19}$ films grown under different tensile stresses. With the increase of tensile strain from 0.23% to 0.62%, the coercive field of the square-shaped loops is changed from 48 to
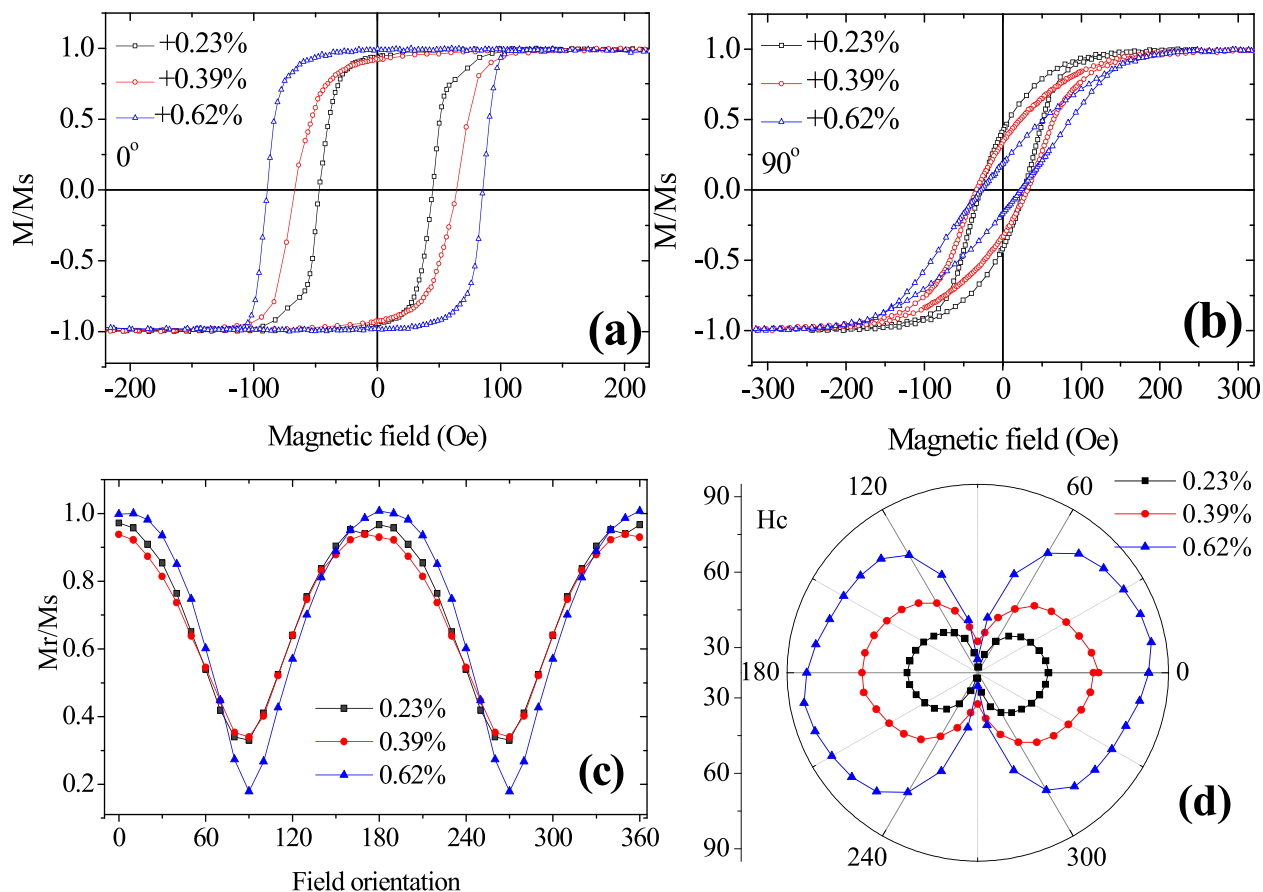
FIG. 3. Representative magnetic hysteresis loops for $Fe_{81}Ga_{19}$/PET with magnetic field applied (a) parallel or (b) perpendicular to the various tensile stresses; (c) Squareness and (d) coercive field versus in-plane field angle for $Fe_{81}Ga_{19}$/PET with different internal stresses.

89 Oe for the field applied along the easy axis ($\varphi = 0°$), and the loop squareness (M_r/M_s) stays constant close to one regardless of the different tensile strains. When the magnetic field orientation is rotated to the hard axis ($\varphi = 90°$), M_r/M_s is decreased from 0.42 to 0.18 with increasing the transverse tensile strain from 0.23% to 0.62%, but the coercive field of hard axis remains unchanged. It can be seen in Fig. 3(c) that the squareness as a function of the field orientation also exhibits a uniaxial symmetry, but the maximum and minimum M_r/M_s appears at $\varphi = 0°$ and $\varphi = 90°$, respectively. The uniaxial anisotropy is enhanced with increasing the tensile stress as indicated by the increase of difference between the maximum and minimum of M_r/M_s. Similarly, the calculated uniaxial anisotropies corresponding to three different samples with tensile strains of 0.23%, 0.39%, and 0.62% are 2.55×10^4, 3.76×10^4, and 6.12×10^4 erg/cm³, respectively. The angular dependence of H_c is presented in Fig. 3(d). The "∞" shaped polar plots of H_c possess a uniaxial symmetry and H_c reaches maximum along the easy axis when the tensile strain is 0.62%.

Our experimental results have demonstrated that magnetic anisotropy of $Fe_{81}Ga_{19}$ film can be mechanically induced by strain growth. The easy axis is parallel to the applied tensile stress, while the hard axis is parallel to the compressive stress. Both the M_r/M_s ratio and coercive field can be tuned by the mechanical stress. The coercivity for magnetic field along the easy axis is increased significantly

with increasing the stress-induced anisotropy. This can be interpreted by considering the increase of strength and density of energy barriers which pin the domain walls. However, when the magnetic field is perpendicular to the easy axis, the effect of compressive stress on H_c is not monotonic.[34]

For all pre-stressed $Fe_{81}Ga_{19}$ films, we notice that the squareness of the hysteresis loop is less than one along the easy axis but higher than zero along the hard axis [see Figs. 2(a) and 2(b) and Figs. 3(a) and 3(b)]. In each magnetic domain, the originally isotropic distributed magnetization will be squeezed into an narrow angle by the applied pre-stress.[35] Therefore, it is viable to speculate that the stress-induced uniaxial anisotropy in polycrystalline $Fe_{81}Ga_{19}$ films does not strictly orient in an identical direction, but has an angle distribution along its average direction. In experiment, the strain resulted from the recovery of bended substrates produces an equivalent uniaxial anisotropy K_e. The total energy for a grain in polycrystalline $Fe_{81}Ga_{19}$ films can be written as: $E = K_e \cos^2(\theta-\delta) - MH \cos(\theta-\varphi)$, where θ is the angle between K_e and the magnetization vector M. We suppose the angle of δ for the distribution of K_e is ranged from $-10°$ to $10°$, using an intermediate value $\delta = 5°$, we obtain the hysteresis loops predicted under various K_e by means of Stoner-Wohlfarth model. As shown in Fig. 4(a), the simulated M_r/M_s as a function of φ possess a uniaxial symmetry about the easy or hard axes. For applying a tensile stress, for
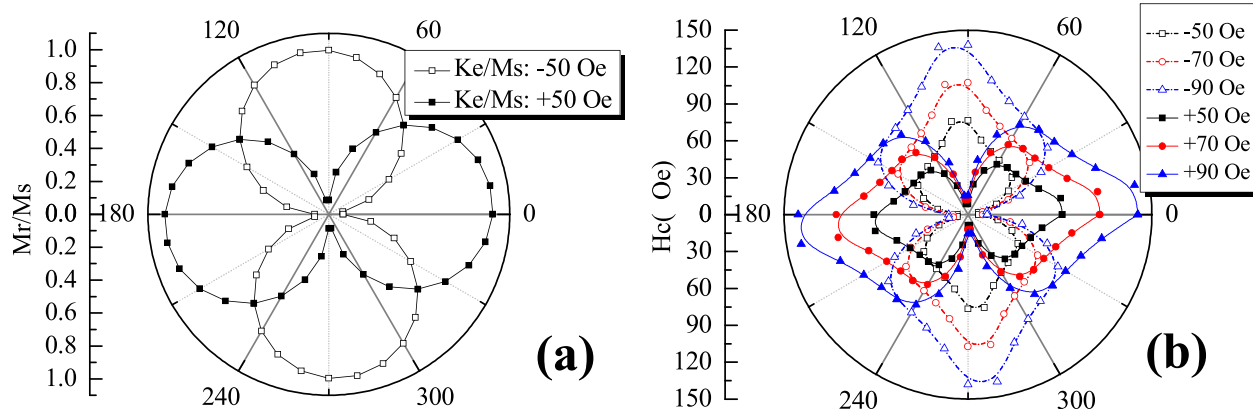
FIG. 4. (a) Polar plots of the normalized remnant magnetization (M_r/M_s) versus in-plane field angle calculated using the modified coherent rotation model under two typical K_e/M_s values of -50 and 50 Oe; (b) Polar plots of coercive field of calculated magnetic hysteresis loops versus in-plane field angle with K_e/M_s of $-50, -70, -90, 50, 70$, and 90 Oe.

example, $K_e/M_s = 50$ Oe, the easy axis is parallel to the tensile stress direction. For applying a compressive stress of $K_e/M_s = -50$ Oe, the easy axis is perpendicular to the compressive stress. The magnetic easy axis of the symmetric polar plots rotates $90°$ when the K_e/M_s is changed from the positive value to the minus one. The angular variations of coercivity for different K_e/M_s are illustrated in Fig. 4(b). It is clear that our experimental observations on pre-stress induced anisotropy for $Fe_{81}Ga_{19}$ films can be explained by the simulations based on the modified Stoner-Wohlfarth model. The calculated results indicate that with increasing K_e/M_s from 50 to 90 Oe, the coercivity is drastically increased from 76 to 184 Oe for the magnetic field along the easy axis, which is larger than the experimental observations. As mentioned above, the effects of stress on the irreversible domain rotation and domain wall movement are quite different, along the easy axis, the energy barrier which pin the domain wall movement is increased with the stress-induced anisotropy; along the hard axis, the effect of compressive stress on the coercive field is not monotonic which cannot be qualitatively predicted by this model. The discrepancy between our experimental observations and the simulated results may arise from the uncertain coefficients used for calculations and the complicated process of irreversible behaviors during magnetization.

In summary, we have investigated the magnetic anisotropy induced by depositing $Fe_{81}Ga_{19}$ film onto the concave/convex PET substrates. The easy axis of stress-induced anisotropy in $Fe_{81}Ga_{19}$ film is parallel to tensile stress. Strain engineering via bowed flexible PET substrate is a viable approach to induce and tune the uniaxial magnetic anisotropy in any direction. The coercive field along the easy axis is increased with increasing the tensile stress and the remanence of hard axis is decreased with the increment of compressive stress. Furthermore, these results clearly demonstrate that magnetoelastic coupling in continuous magnetic films is the source of anisotropy; this is also supported by our modified Stoner-Wohlfarth model simulation. This manipulation of uniaxial anisotropy and coercive field by strain growth is a very useful method for applications of magnetic anisotropy in flexible magnetoelectronic devices.

[1]M. Ali, R. Watts, W. J. Karl, and M. R. J. Gibbs, J. Magn. Magn. Mater. **190**, 199 (1998).
[2]M. Ali and R. Watts, J. Magn. Magn. Mater. **202**, 85 (1999).
[3]J. H. Tan, V. H. Guerrero, R. C. Wetherhold, and W. A. Anderson, *Effect of Stress-induced Magnetic Anisotropy on the Properties of Giant Magnetostrictive Single Layer and Multilayer Thin Films* (MRS Proceedings, 2004), Vol. 855, p. W2.7.
[4]N. Martin, J. McCord, A. Gerber, T. Strache, T. Gemming, I. Mönch, N. Farag, R. Schäfer, J. Fassbender, E. Quandt, and L. Schultz, Appl. Phys. Lett. **94**, 062506 (2009).
[5]E. Quandt and A. Ludwig, J. Appl. Phys. **85**, 6232 (1999).
[6]B. D. Cullity, *Introduction to Magnetic Materials* (Addison-Wesley, Reading, 1972).
[7]J. Shin, S. H. Kim, Y. Suwa, S. Hashi, and K. Ishiyama, J. Appl. Phys. **111**, 07E511 (2012).
[8]X. Y. Xu, M. Li, J. G. Hu, J. Dai, and W. W. Xia, J. Appl. Phys. **108**, 033916 (2010).
[9]B. Özkaya, S. R. Saranu, S. Mohanan, and U. Herr, Phys. Status Solidi A **205**, 1876 (2008).
[10]M. Löhndorf, T. A. Duenas, A. Ludwig, M. Rührig, J. Wecker, D. Bürgler, P. Grünberg, and E. Quandt, IEEE Trans. Magn. **38**, 2826 (2002).
[11]M. Löhndorf, S. Dokupil, J. Wecker, M. Rührig, and E. Quandt, J. Magn. Magn. Mater. **272**, 2023 (2004).
[12]S. Dokupil, M.-T. Bootsmann, S. Stein, M. Löhndorf, and E. Quandt, J. Magn. Magn. Mater. **290–291**, 795 (2005).
[13]M. Brooks, E. Summers, J. B. Restorff, and M. Wun-Fogle, J. Appl. Phys. **111**, 07A907 (2012).
[14]M. Mathews, R. Jansen, G. Rijnders, J. C. Lodder, and D. H. A. Blank, Phys. Rev. B **80**, 064408 (2009).
[15]Q. F. Zhan, S. Vandezande, C. Van Haesendonck, and K. Temst, Appl. Phys. Lett. **91**, 122510 (2007).
[16]D. Garcia, J. L. Muñoz, G. Kurlyandskaya, M. Vazquez, M. Ali, and M. R. J. Gibbs, IEEE Trans. Magn. **34**, 1153 (1998).
[17]D. Garcia, J. L. Muñoz, F. J. Castaño, C. Prados, A. Asenjo, J. M. Garcia, and M. Vazquez, J. Appl. Phys. **85**, 4809 (1999).
[18]M. Melzer, D. Makarov, A. Calvimontes, D. Karnaushenko, S. Baunack, R. Kaltofen, Y. F. Mei, and O. G. Schmidt, Nano Lett. **11**, 2522 (2011).
[19]G. S. Huang and Y. F. Mei, Adv. Mater. **24**, 2517 (2012).
[20]Z. W. Liu, Y. Liu, L. Yan, C. Y. Tan, and C. K. Ong, J. Appl. Phys. **99**, 043903 (2006).
[21]C. Kittel, Phys. Rev. **73**, 155 (1948).

[22]A. E. Clark, J. B. Restorff, M. Wun-Fogle, T. A. Lograsso, and D. L. Schlagel, IEEE Trans. Magn. **36**, 3238 (2000).

[23]G. H. Dai, Q. F. Zhan, Y. W. Liu, H. L. Yang, X. S. Zhang, B. Chen, and R.-W. Li, Appl. Phys. Lett. **100**, 122407 (2012).

[24]V. K. Khanna, J. Phys. D: Appl. Phys. **44**, 034004 (2011).

[25]C. Daboo, R. J. Hicken, E. Gu, M. Gester, S. J. Gray, D. E. P. Eley, E. Ahmad, J. A. C. Bland, R. Ploessl, and J. N. Chapman, Phys. Rev. B **51**, 15964 (1995).

[26]R. P. Cowburn, S. J. Gray, J. Ferré, J. A. C. Bland, and J. Miltat, J. Appl. Phys. **78**, 7210 (1995).

[27]S. M. Zhou, L. Sun, P. C. Searson, and C. L. Chien, Phys. Rev. B **69**, 024408 (2004).

[28]J. Atulasimha and A. B. Flatau, Smart Mater. Struct. **20**, 043001 (2011).

[29]B. W. Wang, S. Y. Li, Y. Zhou, W. M. Huang, and S. Y. Cao, J. Magn. Magn. Mater. **320**, 769 (2008).

[30]D.-H. Han, J.-G. Zhu, and J. H. Judy, J. Appl. Phys. **81**, 340 (1997).

[31]R. A. Kellogg, A. B. Flatau, A. E. Clark, M. Wun-Fogle, and T. A. Lograsso, J. Appl. Phys. **91**, 7821 (2012).

[32]T. Brintlinger, S. H. Lim, K. H. Baloch, P. Alexander, Y. Qi, J. Barry, J. Melngailis, L. Salamanca-Riba, I. Takeuchi, and J. Cumings, Nano Lett. **10**, 1219 (2010).

[33]H. Szymczak, IEEE Trans. Magn. **30**, 702 (1994).

[34]B. Zhu, C. C. H. Lo, S. J. Lee, and D. C. Jiles, J. Appl. Phys. **89**, 7009 (2001).

[35]I. J. Garshelis, J. Appl. Phys. **73**, 5629 (1993).